Type Ia Supernovae Detection Rates for LSST

Pinaki Roy
Visiting Project Student (VSP)

supervised by
Surhud More, Anupreeta More

Inter-University Centre for Astronomy and Astrophysics (IUCAA)
Pune, Maharashtra, India

October-December 2018

1 Introduction

The purpose of the project was to study the scope of the color-magnitude plot technique in identifying gravitationally lensed (g-lensed) Type Ia Supernovae (SNe Ia), that was proposed in [10] in the context of an apparently superluminous supernova (SLSN), PS1-10afx at a redshift of 1.388, and concluding that it was a normal SNe whose brightness had been magnified by a lensing galaxy at a redshift of 1.117. The work looks at the feasibility of this technique in distinguishing between g-lensed SNe Ia and SLSNe amongst the known $\sim$40 SLSN candidates. Many of these candidates have been classified as SLSN-I, SLSN-II or SLSN-R as per [3] with some uncertainties. Some candidates remain poorly understood and hence subjected to innovative speculations such as lensing by a foreground object that may explain some of the observed peculiarities.

2 Method

Typically an r-i (observed) vs i (observed) color-magnitude plot is prepared and it can be seen that the most of the supernovae lie below an apparent critical line (at near maximum) as illustrated in Figure 1. A few that lie above (or on) the bold line are either contaminants (not g-lensed SNe Ia) or believed to be g-lensed SNe Ia (like PS1-10afx and iPTF-16geu). The technique also requires the rise time color-magnitude to consistently exceed the threshold. This condition sieves out much of the contaminants that occasionally surpass the limit. Moreover, the plot shows an upward (color excess) and rightward (decreasing magnitude) displacement of supernovae of the same class (say, Type Ia) with increasing redshift (distance) due to the $(1 + z)$ delay factor so that the rest frame bands appear redder when observed. Hence, the u-band (365 nm) will become z-band (900 nm) for a redshift of $\sim$1.5.

We plotted all the hitherto known SLSNe (with sufficient photometry data published), a sample of SNe Ia and core-collapse supernovae (CC SNe) observed by various missions at different redshifts, and found some outliers besides PS1-10afx that is already discussed in Quimby et al. (2014). We then checked for possible causes for their uncommon color excess viz. their situation (central or peripheral) in their respective host galaxies (if known). We could attribute to this the offset of the SNe Ia SNLS-03D4cx. About the SL SNe (other than PS1-10afx) that show offsets, this cause cannot be cited with confidence as their host-galaxies are inadequately described.

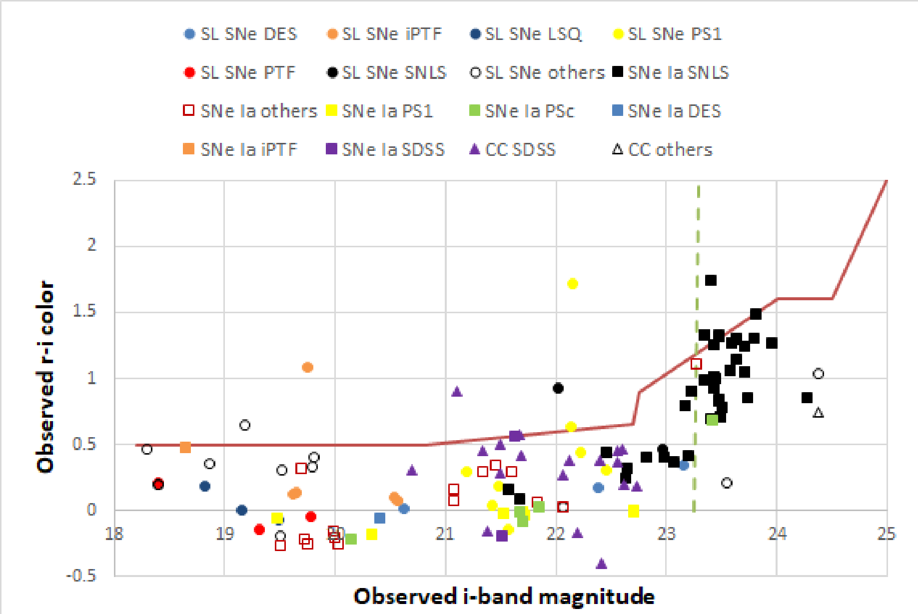

Figure 1: Color-Magnitude plot for a sample of supernovae

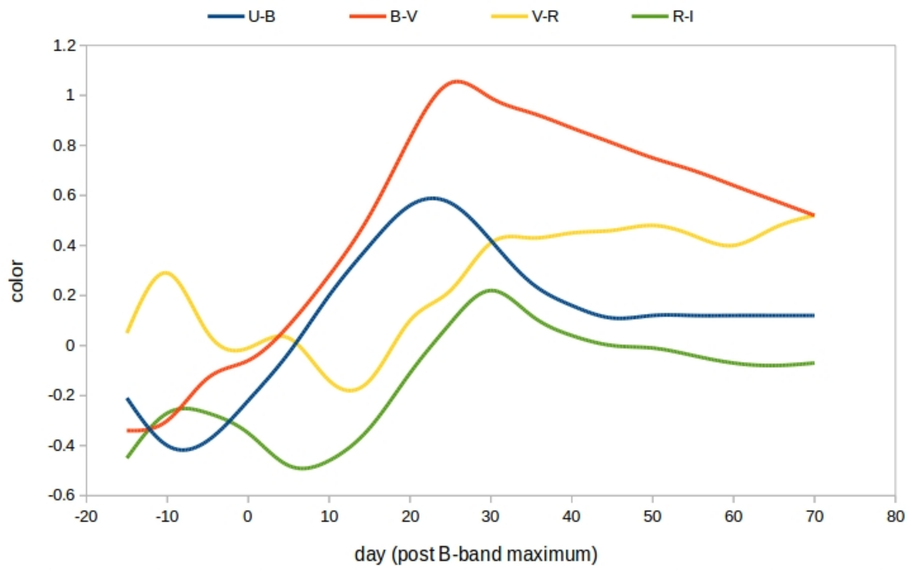

Figure 2: Color evolution for type Ia supernovae [8]

3 Predicting Type Ia Supernova Detection Rates for LSST

The Large Synoptic Survey Telescope (LSST) is a wide-field survey reflecting telescope with an 8.4-meter primary mirror, coming up in Chile (first light expected in 2019), equipped with a 3.2 Gigapixel CCD imaging camera that will photograph the entire available sky every few nights. With a very wide field of view (3.5 deg in diameter, or 9.6 deg^2). LSST will cover about 18,000 deg^2 of the southern sky with 6 filters (UGRIZY covering 350 to 1060 nm wavelengths) in its main survey spanning 10-12 years, with about 825 visits to each spot. The magnitude limits are expected to be $r < 24.5$ in single images, and $r < 27.8$ in the full stacked data.

Table 1: LSST filter passbands

Filter	u	g	r	i	z	y
Wavelength range (nm)	350-400	400-552	552-691	691-818	818-922	948-1060

The number of visits and the (5σ) limiting apparent magnitude in each band for the point sources for one year and ten years of the running survey are listed in [4]

Table 2: One year of observation

	u	g	r	i	z	y
Number of visits	5	8	18	18	16	16
$m_{5\sigma}$	24.9	26.2	26.4	25.7	25.0	23.7

Table 3: Ten years of observation

	u	g	r	i	z	y
Number of visits	56	80	184	184	160	160
$m_{5\sigma}$	26.1	27.4	27.5	26.8	26.1	24.9

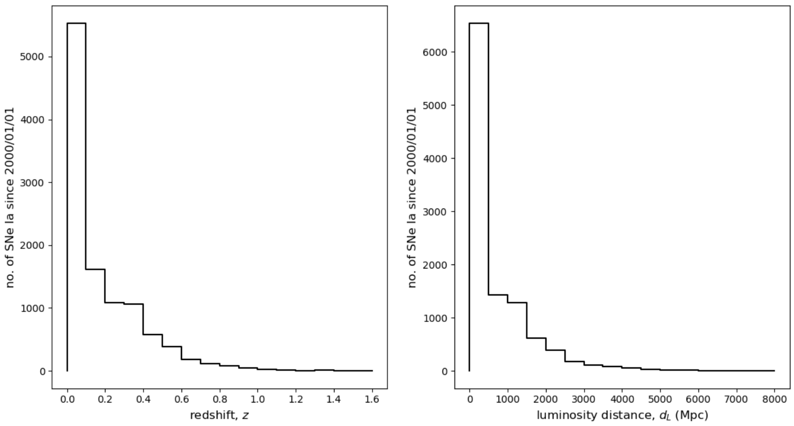

Figure 3: (a) SNe Ia detection vs Redshift (b) SNe Ia detection vs Luminosity distance

3.1 K-correction (Bandpass shifting)

The observed apparent P-band magnitude of a source, m_Q, is related to the emitted-frame absolute Q-band magnitude as:

$$m_Q = M_P + \mu + K_{PQ} + A_P + A_Q$$

where distance modulus, $\mu = 5\log_{10}\left(\frac{d_L}{10\text{pc}}\right)$ where d_L is the luminosity distance. K_{PQ} is the K-correction. A_P and A_Q are extinctions in host galaxy and our galaxy respectively; the former is usually not accounted for while specifying supernova absolute magnitudes.

P and Q are related as:

$$\lambda_Q = (1+z)\lambda_P \implies \nu_P = (1+z)\nu_Q$$

Note that the two wavelengths may belong to the same band in the source frame (rest frame) and the observer frame if the redshift is small in which case the K-correction will be denoted by K_{PP}. The K-correction (for SN Ia) calculations require the SED (equivalently, the spectral template time series) of the SN Ia, and this dependence is large at redshifts where the observed and the rest-frame filters are misaligned. The K-corrections are primarily driven by SN Ia colors and spectral features.[7]

The relation between luminosity distance, d_L and redshift, z, for a spatially flat ΛCDM universe is

$$d_L = (1+z)d_C, \text{ where comoving distance, } d_C = d_H \int_0^z \frac{dz'}{\sqrt{W(z')}}, \text{ and Hubble distance, } d_H = \frac{c}{H_0}$$

and $W(z') = \Omega_R(1+z)^4 + \Omega_M(1+z)^3 + \Omega_\Lambda$ and $\Omega_R + \Omega_M + \Omega_\Lambda = 1$. H_0 is the value of the Hubble parameter, $H = \dfrac{\dot{a}}{a}$ at the current epoch, $a(t)$ being the dimensionless cosmic scale factor. In contrast, the angular diameter distance for a spatially flat ΛCDM universe is given by $d_A = \dfrac{d_C}{1+z}$

Evidently, the relationship between the luminosity distance of standard candles and the angular-diameter distance is

$$d_L = (1+z)^2 d_A \quad \text{(Etherington's distance-duality equation)}$$

For a more detailed description (and depiction) of the various cosmological distance measures and their respective dependence on redshift, see [5].

Following [6], the K-correction can be expressed as

$$K_{PQ} = -2.5\log_{10}\left[(1+z)\frac{\int \frac{d\nu_o}{\nu_o} f(\nu_o)Q(\nu_o)}{\int \frac{d\nu_e}{\nu_e} f(\frac{\nu_e}{1+z})P(\nu_e)} \times \frac{\int \frac{d\nu_e}{\nu_e} g_\nu^P(\nu_e)P(\nu_e)}{\int \frac{d\nu_o}{\nu_o} g_\nu^Q(\nu_e)Q(\nu_o)}\right]$$

3.2 Preparatory considerations

Q: If the B-band peak of an SN Ia is $M_B = -19.3$ and its redshift, $z = 1.5$, what will be the apparent magnitude in the filter in which this peak will be seen?
A: The B-band peak will be seen in the J-band due the $(1+z)$ delay factor. The luminosity distance for $z = 1.5$ comes to 7817.2 Mpc. Using the distanceequation discussed above, and neglecting the K-correction extinction, the J-band apparent magnitude, $m_J = 25.2$

Ignoring the gap between z- and y- passbands, and assuming the type Ia supernova in its rest frame emits only in "*ugrizy*" range, the limiting redshifts (redshift upto which a passband may "capture" the supernova) may be calculated (by virtue of $(1+z)$ dilation) as (u-band lower cut-off)$\times(1+z)$ =(passband upper cut-off). Also, noted are the typical type Ia absolute magnitudes in these passbands (using the template given in [8] and taking $M_B = 19.25$).

Table 4: Limiting redshifts of filters for ideal SN Ia

Filter	u	g	r	i	z	y
Limiting redshift, z_{lim}	0.143	0.577	0.974	1.337	1.634	2.028
SN Ia absolute magnitude, M	-19.47	-19.19	-19.08	-19.05	–	–
Absolute magnitude at z_{lim} using Table[2], z_{view}	-13.5	-15.7	-16.9	-18.5	-19.7	-21.6
Revised limiting redshift, z_{lim}	0.143	0.577	0.974	1.337	1.503	0.930

From Table[4], it is apparent that LSST can detect the UV peak of normal SNe Ia upto $z = 1.5$

[2] & [12] gives the peak B-band magnitudes (M_B) and corresponding dispersion of Type Ia SNe assuming $H_0 = 70$ km/s/Mpc and a cosmology with $\Omega_M = 0.3$ and $\Omega_\Lambda = 0.7$. The weighted mean M_B comes to -19.12 and the weighted dispersion, $\sigma = 0.43$

Table 5: SNe Ia Types

Type	M_B	σ	f
Ia bright	-19.6	0.30	0.20
Ia normal	-19.3	0.45	0.64
Ia faint	-17.8	0.50	0.16

[9] gives the luminosity function (in terms of B-band absolute magnitude, M) for Type Ia as:

$$\frac{d\Phi_X}{dM} = \frac{n_X(z)}{(1+z)} \frac{1}{\sqrt{2\pi}\sigma} \exp\left[-\frac{(M - M_X^*)^2}{2\sigma_X^2}\right] \tag{1}$$

For supernova type, $X =$Ia, using $M_{\mathrm{Ia}}^* = -19.25$ and $\sigma_{\mathrm{Ia}} = 0.5$ [11], eqn (1) becomes:

$$\frac{d\Phi_{\mathrm{Ia}}}{dM} = \frac{n_{\mathrm{Ia}}(z)}{(1+z)} (0.8) \exp\left[-\frac{(M + 19.25)^2}{0.5}\right] \tag{2}$$

where SN Ia rate ([9]), $n_{\mathrm{Ia}} = \left(1.028 \times 10^{-3} M_\odot^{-1}\right) \dfrac{\displaystyle\int_{0.1}^{t(z)} \rho_{\mathrm{SFR}}[z(t - t_{\mathrm{D}})] f(t_{\mathrm{D}})\, dt_{\mathrm{D}}}{\displaystyle\int_{0.1}^{t(z=0)} f(t_{\mathrm{D}})\, dt_{\mathrm{D}}}$

The delay time distribution (DTD) of SNe Ia, $f(t_{\mathrm{D}}) \propto t_{\mathrm{D}}^{-1.08}$ ($t_{\mathrm{D}} > 0.1\,\mathrm{Gyr}$) so that

$$n_{\mathrm{Ia}} = \left(1.28 \times 10^{-3} M_\odot^{-1}\right) \frac{\displaystyle\int_{0.1}^{t(z)} \rho_{\mathrm{SFR}}[z(t - t_{\mathrm{D}})]\, t_{\mathrm{D}}^{-1.08}\, dt_{\mathrm{D}}}{\displaystyle\int_{0.1}^{t(z=0)} t_{\mathrm{D}}^{-1.08}\, dt_{\mathrm{D}}}$$

The cosmic star formation rate (empirical)[9], $\rho_{\mathrm{SFR}}(z) = \dfrac{(0.0118 + 0.08z)h}{1 + (z/3.3)^{5.2}}\ \left[M_\odot \mathrm{yr}^{-1} \mathrm{Mpc}^{-1}\right]$

where dimensionless hubble parameter, $h = \dfrac{H_0}{100\,\mathrm{km\,s^{-1}Mpc^{-1}}} = 0.7$

The numerator in the expression for SN Ia rate requires the evaluation of the star formation rate expression with the redshift, z, stated as a function of $(t - t_D)$. This may be achieved conveniently by putting, $z = \left(\sqrt{\dfrac{28}{t\,(\text{in Gyr})} - 1} - 1\right)$ which is obtained by virtue of the formula, $t = \dfrac{1\,\mathrm{Gyr}}{1 + (1+z)^2}$ derived in [1] and using $H_0 = 70$ km/s/Mpc.

3.3 Crunching numbers

Multiply the SN Ia rate by the differential comoving volume at each redshift to obtain the number of SN Ia per year at that redshift. This should be further reduced by a factor of $(1 + z)$ to account for cosmological time dilation. Moreover, since the LSST in a year covers 18000 deg^2 sky area which is 43.633% of the total area (41253 deg^2) of the sky, the number of SNe Ia per year for LSST to detect needs to be reduced to 0.43633 of its value. If instead of the LSST sky, estimate is to be made only for the field of view (FOV) which is 9.6 deg^2, the factor will be 0.0002327 instead of 0.43633. For the number of SNe Ia thus found, the spectral flux epoch t the appropriate e is determined from the Hsiao (rest-frame) spectral templates, and the corresponding absolute magnitude is determined in the concerned filter after applying redshift correction to the spectra. Then the apparent magnitude is obtained which is then compared with the LSST limiting magnitude for the chosen filter to decide the detectability. Thus the counting is performed. The results are of this process for g and i filters are shown in Figure 7. This estimate does not take dust extinction into account. The LSST cadence is accounted for by restricting the observations to periodically spaced dates in a year.

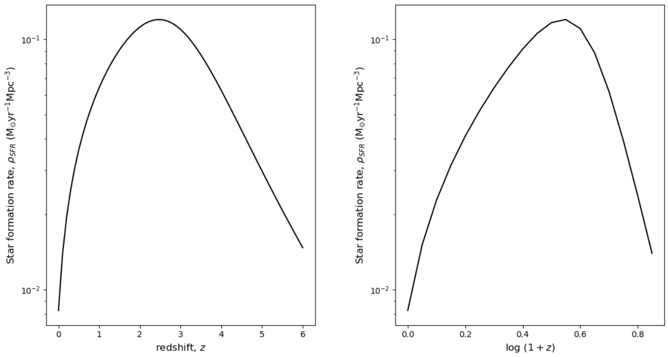

Figure 4: Cosmic Star Formation Rate vs Redshift

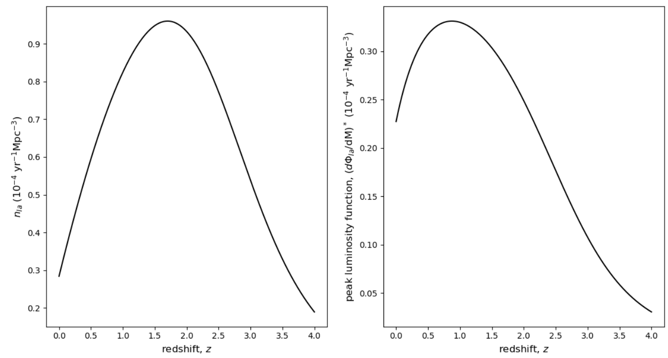

Figure 5: (a) SNe Ia rate vs Redshift (b) Peak luminosity function vs Redshift

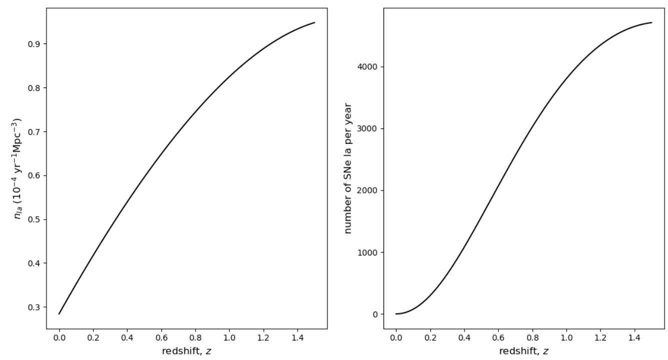

Figure 6: (a) SNe Ia rate vs Redshift (b) Number of SN Ia occurring per year

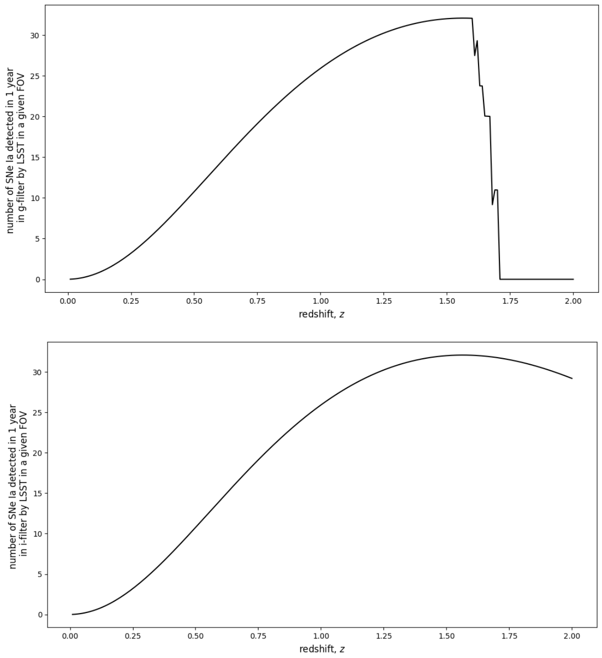

Figure 7: SNe Ia detections by LSST in a year in a fixed FOV in (a) g-filter (b) i-filter

References

[1] M. Carmeli, J. G. Hartnett, and F. J. Oliveira. The Cosmic Time in Terms of the Redshift. *Foundations of Physics Letters*, 19:277–283, April 2006.

[2] T. Dahlen et al. High-Redshift Supernova Rates. *APJ*, 613:189–199, September 2004.

[3] A. Gal-Yam. Luminous Supernovae. *Science*, 337:927, August 2012.

[4] A. Gorecki et al. A new method to improve photometric redshift reconstruction. Applications to the Large Synoptic Survey Telescope. *AAP*, 561:A128, January 2014.

[5] D. W. Hogg. Distance measures in cosmology. *ArXiv Astrophysics e-prints*, May 1999.

[6] D. W. Hogg, I. K. Baldry, M. R. Blanton, and D. J. Eisenstein. The K correction. *ArXiv Astrophysics e-prints*, October 2002.

[7] E. Y. Hsiao, A. Conley, D. A. Howell, M. Sullivan, C. J. Pritchet, R. G. Carlberg, P. E. Nugent, and M. M. Phillips. K-Corrections and Spectral Templates of Type Ia Supernovae. *APJ*, 663:1187–1200, July 2007.

[8] P. Nugent, A. Kim, and S. Perlmutter. K-Corrections and Extinction Corrections for Type Ia Supernovae. *PASP*, 114:803–819, August 2002.

[9] M. Oguri and P. J. Marshall. Gravitationally lensed quasars and supernovae in future wide-field optical imaging surveys. *MNRAS*, 405:2579–2593, July 2010.

[10] R. M. Quimby et al. Detection of the Gravitational Lens Magnifying a Type Ia Supernova. *Science*, 344:396–399, April 2014.

[11] D. Richardson, R. L. Jenkins, III, J. Wright, and L. Maddox. Absolute-magnitude Distributions of Supernovae. *AJ*, 147:118, May 2014.

[12] J. L. Tonry et al. Cosmological Results from High-z Supernovae. *APJ*, 594:1–24, September 2003.